[8]A. M. Cantu, W. H. Parkinson, G. Tondello, and G. P. Tozzi, J. Opt. Soc. Am. 67, 1030 (1977).
[9]D. Rassi, V. Pejcev, and K. J. Ross, J. Phys. B 10, 3535 (1977).
[10]P. Ziem, R. Bruch, and N. Stolterfoht, J. Phys. B 8, L480 (1975).
[11]R. L. Kelly, U. S. Naval Research Laboratory Report No. 6648, 1968 (unpublished) (U. S. GPO, Washington, D. C.).
[12]S. E. Harris, Appl. Phys. Lett. 31, 498 (1977).
[13]L. J. Zych, J. Lukasik, J. F. Young, and S. E. Harris, Phys. Rev. Lett. 40, 1493 (1978).

Electron Energy Transport into Layered Targets Irradiated by CO_2-Laser Light

J. C. Kieffer, H. Pépin, F. Martin, P. Church, and T. W. Johnston
Institut National de la Recherche Scientifique–Energie, Université du Québec, Varennes, Québec J0L2P0, Canada

and

R. Decoste
Institut de Recherche d'Hydro-Québec, Varennes, Québec J0L2P0, Canada
(Received 22 January 1980)

Inward energy transport ranges in layered targets have been measured as a function of the irradiance of short-pulse CO_2-laser light. As electromagnetic ponderomotive effects become important, the penetration of thermal electrons is sharply reduced and the penetration of suprathermal electrons increases much more slowly with irradiance. These results are discussed in the context of target implosions driven by suprathermal electrons.

PACS numbers: 52.50.Jm

Efficient energy transport from the absorption region to the core of the pellet shell target is needed in laser fusion to produce the inward shell acceleration and subsequent thermonuclear-burn conditions. Sufficient energy transport by thermal electrons has been demonstrated for 1.06-μm lasers at moderately low irradiance.[1] Longer-wavelength lasers, however, produce abundant suprathermal electrons leaving much less energy available for thermal electron transport. It has then been suggested that the hot-electron penetration into the target could become an alternate energy transport mechanism for 10.6-μm lasers at high target irradiance.[2] Lateral transport of hot electrons has been observed[3] with a 10.6-μm-wavelength laser at somewhat higher irradiances than ours, but we do not address that problem here. In this Letter, we report observations of the depth of heat transport by both thermal and suprathermal electrons for two different irradiance regimes. At the lower irradiances, both the thermal- and suprathermal-electron penetration are increasing with irradiance, as expected. However, at the higher irradiances, with the onset of electromagnetic ponderomotive force effects, the thermal-electron penetration decreases sharply while the suprathermal-electron penetration increases only weakly with irradiance. These results are encouraging for the fusion application mentioned above.

These experiments were carried out with a CO_2-laser beam (10.6 μm wavelength) incident on planar layered targets. The *S*-polarized laser pulse, 1.5 nsec in duration (full width at half maximum) with a prepulse-to-main-pulse contrast ratio $<10^{-6}$, was focused on target by an $f/1.5$ off-axis parabolic mirror. With an infrared film sensitizing technique,[4] the half-energy spot diameter was measured to be 130 μm, essentially independent of laser irradiance and without any hot spots.

To ascertain the importance of the electromagnetic ponderomotive force effects on the transport and interaction physics, we covered the range of target irradiance corresponding to a variation of the parameter $\gamma = v_0/v_t$ (electron oscillatory to cold thermal velocity) from 0.2 to 1.5. This range covers the transition from a regime of "weak" ($\gamma < 1$) to "moderate" ($\gamma > 1$) plasma-density profile modification.[5] This transition is clearly illustrated in Fig. 1 by typical interferograms obtained with a 35-psec ruby-laser pulse synchronized and time delayed with respect to the CO_2 laser. At lower irradiances ($\gamma < 1$), Abel inversion of the well-separated fringes yields an on-axis density-gradient scale length of about 35 μm. At higher irradiances ($\gamma > 1$), the density scale length is reduced to less

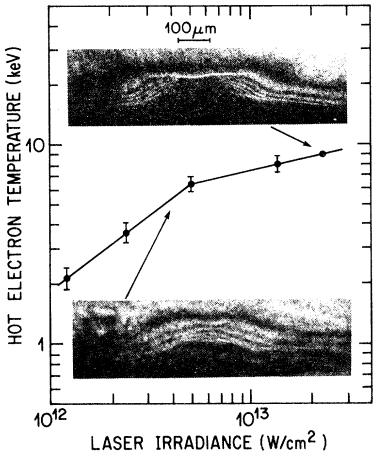

FIG. 1. Ponderomotive force effects on the hot-electron temperature and the plasma density profile. The interferograms were taken near the peak of the laser pulse at the average irradiances indicated by the arrows.

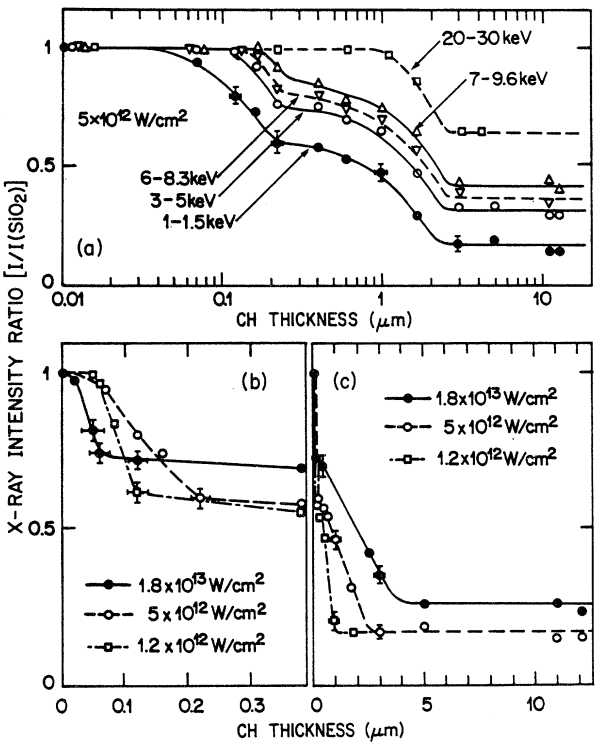

FIG. 2. X-ray intensities vs $(CH)_x$ overlayer thickness, normalized to the emission from pure SiO_2 glass substrate. (a) Relative behavior of various x-ray channels at a given irradiance. (b) Transitions from steep to slow x-ray variation with increasing $(CH)_x$ thickness for three laser irradiances. (c) X-ray-intensity saturations with increasing thickness on an extended linear scale. The error bard reflect the ± 5% shot-to-shot reproducibility resulting in a ± 10% uncertainty for the ratios of two independent shots.

than 10 μm, as can be seen from the closely spaced fringes on axis. The ponderomotive steepening of the density gradient coupled with the resonant absorption mechanism give rise to various other changes in plasma behavior.[6,7] Among others, the scaling of the hot-electron "temperature" with irradiance[5] is modified above a critical irradiance, as can be seen in Fig. 1. This hot-electron temperature is inferred from continuum x-ray spectra measured from irradiated targets with filter-absorber detectors covering the 1–50-keV range.[6] Strong profile steepening[8] and changes of the hot-electron temperature scaling[5] have also been reported elsewhere. We will see next that the inward energy transport changes in important ways above and below the critical irradiance.

The electron energy transport ranges are inferred from the variation of the x-ray emission from planar layered targets[9] as a function of layer thickness. The targets consisted of a thin layer of polystyrene $[(CH)_x]$ deposited on a glass (SiO_2) substrate. Continuum x-ray emission from the glass substrate provides quantitative evidence of the effectiveness of energy transport through the relatively weakly emitting $(CH)_x$ overlayer. Figure 2(a) shows the x-ray intensities, normalized to the bare glass substrate emission, for various channels as a function of the overlaid plastic thickness, at a given irradiance. No x-ray contribution from the glass substrate is observed on any channels for plastic thickness more than about 2 μm at that irradiance. As expected, the x-ray contribution from the glass substrate increases with decreasing $(CH)_x$ thickness. Notice, however, for all channels, the change in the x-ray intensity dependence with $(CH)_x$ thickness when the plastic layer is reduced below 0.2 μm.

Figures 2(b) and 2(c) show typical normalized x-ray responses versus $(CH)_x$ thickness for different laser intensities, on linear scales. Although only the Be channel (1–1.5 keV) is represented here, other channels have similar behavior, as demonstrated in Fig. 2(a), at a given laser irradiance. The change in the x-ray intensity dependence with increasing plastic thickness is now more apparent in Fig. 2(b). This transition from steep to slow x-ray variation varies with the laser irradiance. Figure 2(c) shows the x-ray intensity saturation with increasing plastic thickness on an extended linear scale. This transition

to x-ray emission from thick plastic is shifted to higher overlayer thickness with higher laser irradiance.

The first transition in the x-ray behavior [Fig. 2(b)] may be related to the penetration of a heat wave into the material by electron thermal conduction during the laser pulse. The thermal penetration depth is then the $(CH)_x$ thickness which is sufficient to reduce substantially the thermal heating of the glass substrate and above which the x-ray emission decreases more slowly. In a similar experiment,[10] at a laser irradiance of 3×10^{13} W cm^{-2}, a thermal penetration depth consistent with our results has been measured in Al, with plasma line radiation instead of continuum emission.

The second x-ray transition corresponding to the beginning of pure $(CH)_x$ emission [Fig. 2(c)] is related to the penetration of suprathermal electrons in the material. The $(CH)_x$ thickness which is sufficient to prevent substantial x-ray emission due to energetic electrons decelerated in the SiO_2 substrate is called the suprathermal penetration depth. Previous work[10,11] has been done on the range of fast electrons in solid targets using $K\alpha$ radiation from underlying material.

Figure 3 shows the behavior of both the thermal- and suprathermal-electron penetration depths as a function of the laser irradiance. The appearance of two different irradiance regimes, discussed above from Fig. 1, with a critical irradiance around 5×10^{12} W/cm^2, is also evident in Fig. 3. Below the critical flux, at the lower irradiances, both the thermal- and suprathermal-electron penetration are increasing with irradiances. Above the critical flux, however, the thermal-electron penetration actually *decreases* sharply while the suprathermal-electron penetration increases much more slowly with irradiance than before.

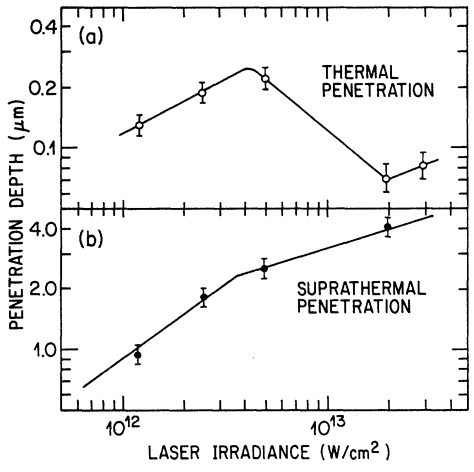

FIG. 3. (a) Thermal- and (b) suprathermal-electron penetration depths as a function of the laser irradiance. Notice the two distinct irradiance regimes already identified in Fig. 1 with about the same critical irradiance.

Free-standing foil burnthrough depths were also deduced from the saturation of the x-ray emission from irradiated thin plastic foils. We find fairly good agreement between thermal penetration depths inferred from layered targets and those inferred from free-standing foils. X-ray emission from free-standing thick foils and thick layers are the same. (Penetration results from foils should be treated with caution since foil acceleration before the plasma becomes subcritical may affect the transport physics.)

In order to determine whether the reduced thermal penetration above the critical irradiance is due to reduced heat transport or due to reduced absorbed energy, the fractional absorption of the incident laser energy was measured over the laser irradiance regime covered in Fig. 3. Calorimetry measurements of the expanding plasma give a fractional absorption independent of the laser irradiance of about 30%, in relatively good agreement with other measurements.[12] One may then be tempted to claim evidence of strong inhibition of heat transport by thermal electrons above the critical irradiance through one or more of the usual mechanisms such as acoustic turbulence[13] and magnetic fields.[14] On the other hand, this ponderomotive steepening of the density gradient coupled with the resonant absorption mechanisms could be such that less absorbed laser energy is available to thermal electrons and more for production of energetic electrons. Thus the dramatic change in the thermal electron penetration in Fig. 3(a) could be accounted for by heat transport inhibition *and/or* reduction of the energy in thermal electrons.

The range of suprathermal penetration depth reported in Fig. 3 is consistent with electrons at energies of tens of kiloelectronvolts, decelerated within a few microns of solid plastic.[15] Actually, as we see below, the deceleration region of the fast electrons is likely to be a plasma of complex density and temperature profiles evolving in time. The collisionless energy transport, from the critical layer where the hot electrons are produced to the collisional absorption region of the electrons, implies bulk heating of the decel-

eration region. A crude estimate of the amount of energy transported and deposited into the deceleration region can be obtained from the suprathermal component of the absolute x-ray spectrum measured from irradiated thick $(CH)_x$ targets. At an irradiance of 3×10^{13} W cm^{-2} with a 1.5-nsec pulse, about 30% of the absorbed laser energy goes via fast electrons deep into the target.[6] We estimate that carbon ions with directed average velocities around 10^7 cm/sec are produced when the heat from the fast-electron deceleration within the measured $(CH)_x$ thickness is converted chiefly into directed kinetic energy of expansion. For a sufficiently long laser pulse, a steady-state situation similar to the ablation observed for long 1.06-μm laser pulses is also possible.[16,1]

Hot-electron preheat inside laser fusion targets is unwanted and copious hot electrons are known to be produced at the high values of $I\lambda^2$ ($\gtrsim10^{16}$ W cm^{-2} μm^2) attained by powerful CO_2 lasers. It has been proposed[2] to make use of the hot-electron absorption in a thick shell of low-Z material as a driving mechanism for the shell compression, hopefully attaining interestingly low ablation velocities as indicated above. In that connection, the slower increase of fast-electron penetration depth with irradiance at the higher levels ($\sim I^{0.3}$) shown in Fig. 3(b) (presumably due to the slow increase of fast-electron temperature) means that dismayingly thick shells may not be required. For instance, extrapolating to 10^{16} W/cm^2 of CO_2-laser irradiance suggests that one would only need about 25 μm of polystyrene.

To conclude, at high irradiance levels ($I\lambda^2$ $\gtrsim 10^{15}$ W cm^{-2} μm^2) the thermal-electron penetration is reduced with a dramatic change near the critical irradiance. Furthermore, the fast-electron penetration increases relatively more slowly ($\sim I^{0.3}$) than at lower levels ($\sim I^{0.75}$), an encouraging result for the idea[2] of using hot-electron transport in laser fusion.

The authors wish to acknowledge the continuing excellent technical support of J. Gauthier, P. P. Mercier, F. Poitras, and J. G. Vallée. This research was supported by the Natural Sciences and Engineering Research Council of Canada.

[1]R. Decoste *et al.*, Phys. Rev. Lett. 42, 1673 (1979); B. H. Ripin *et al.*, Phys. Rev. Lett. 43, 350 (1980).

[2]R. J. Fries *et al.*, LASL Report No. LA UR 79 761, 1979 (unpublished); M. H. Key, in Proceedings of the Twentieth Scottish Universities Summer School, St. Andrews, 1979, edited by R. A. Cairns and J. J. Sanderson (Scottish Universities Summer Schools in Physics Publications, to be published).

[3]N. A. Ebrahim *et al.*, Phys. Rev. Lett. 43, 1995 (1979).

[4]G. Mitchel *et al.*, Appl. Opt. 18, 2422 (1979).

[5]D. W. Forslund, J. M. Kindel, and K. Lee, Phys. Rev. Lett. 39, 284 (1977).

[6]H. Pépin *et al.*, J. Appl. Phys. 50, 6784 (1979).

[7]G. Mitchel *et al.*, in *Proceedings of the IEEE International Conference on Plasma Science, Montreal, Canada, 1979* (IEEE, New York, 1979), p. 89.

[8]R. Fedosejevs *et al.*, Phys. Rev. Lett. 39, 932 (1977); D. T. Attwood *et al.*, Phys. Rev. Lett. 40, 184 (1978).

[9]F. C. Young *et al.*, Appl. Phys. Lett. 30, 45 (1977); B. Yaakobi and T. C. Bristow, Phys. Rev. Lett. 38, 350 (1977).

[10]K. B. Mitchell and R. P. Godwin, J. Appl. Phys. 49, 3851 (1978).

[11]J. D. Hares *et al.*, Phys. Rev. Lett. 42, 1216 (1979).

[12]D. M. Villeneuve *et al.*, J. Appl. Phys. 50, 3921 (1979).

[13]W. M. Manheimer and D. G. Colombant, Phys. Fluids 21, 1818 (1978).

[14]J. A. Stamper, E. A. McLean, and B. H. Ripin, Phys. Rev. Lett. 40, 1177 (1978); A. Raven, O. Willi, and P. T. Rumsby, Phys. Rev. Lett. 41, 554, 1002(E) (1978).

[15]L. Valentin, *Physique Subatomique* (Hermann, Paris, 1975), p. 138; R. D. Evans, *The Atomic Nucleus* (McGraw-Hill, New York, 1955), p. 622.

[16]M. K. Matzen and R. K. Morse, Phys. Fluids 22, 654 (1979).

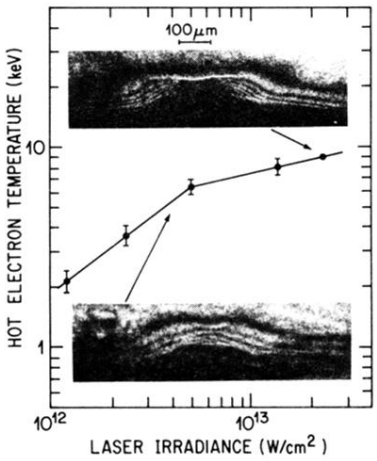

FIG. 1. Ponderomotive force effects on the hot-electron temperature and the plasma density profile. The interferograms were taken near the peak of the laser pulse at the average irradiances indicated by the arrows.